Analyzing the Power System in the Presence of DC Link and FACTs Controllers

K. Sri Kumar [1], Ch.V.Suresh[2]

1 Department of EEE, University College of Engineering, JNTUK, Kakinada.

2 Department of EEE, Vasireddy Venkatadri Institute of Technology, Nambur, Guntur.

Abstract

At present, DC power transmission systems have been integrated into existing power systems. Unlike utility ac/dc power systems, industrial power systems are characterized by multi-terminal dc systems which supply distributed dc motor loads. The principal tool used in designing these systems is the load-flow program. Load-flow analysis techniques developed to date which are suitable for ac/dc power-systems analysis invariably invoke the assumption that the direct-current commutation-resistance product (IdRc) is small compared to the ac system voltage. Power losses in the grid are important, and as the power losses decrease the efficiency increases. Not much research has been done recently on the Newton-Raphson Power Flow (NRPF) method in polar form for systems with High Voltage Direct Current (HVDC) subsystems. Similarly, application of power electronic based controllers namely flexible AC transmission system (FACTs) controllers have been installed to increase the flexibility in power system operation and control. The presented methodology is tested on IEEE-14 bus system in the presence of FACTs controllers such as Static VAr compensator (SVC) and thyristor controlled series compensator (TCSC) with supporting numerical and graphical results.

Keywords: AC-DC load flow; TCSC; SVC; Transmission efficiency; Corona loss.

1. Introduction

Electrical power systems are designed to serve the needs of real and reactive power, as demanded by various connected loads in the network. Load flow studies are necessary to determine the steady-state solution of a power system network at a given set of Bus-bar loads. In today's high technology age, the demand for electricity continues to increase. Due to the rapid growth in demand for electricity, electric power systems are becoming increasingly extensive and their control is becoming ever more complex. In addition, a guaranteed electricity supply is a necessity for industrial growth as well as in other areas of human activity.

To that end, power industry planners are demanding the provision of higher quality electrical power. This requires improving system security and its environmental impact, in tandem with the pursuit of greater efficiency. However, the criterion of perfection is never met because there are consistent differences between the model and reality.

The power flow problem is solved by determining the values of steady-state complex voltages at all buses of the network, from which the active and reactive flows in every transmission line are calculated. Because the equations representing the power system are nonlinear, the well-established nodal properties of the power network and equipment are utilized in power flow solution methods. In its most basic form, these equations are

derived by assuming that a perfect symmetry exists between the phases of the three-phase power system. Due to the nonlinear nature of the power flow equations, an iterative process obtains the numerical solution.

Recently, there have been considerable advances in High Voltage Direct Current (HVDC) technology as a feasible option. Therefore, load flow analysis techniques have to be extended to deal with such mixed HVDC systems. The integration of DC links or HVDC networks into AC systems is achievable and can be advantageous in certain applications such as bulk power transmission, AC network interconnections, and reinforcing AC networks.

Load flow analysis is the most important and fundamental tool applied to a power system to investigate problems in power system operations and planning. It analyzes the power systems in normal steady-state operation using simplified notation, such as a one-line diagram and per-unit system. The power flow problem consists of a given transmission network where all lines are represented by a Pi-equivalent circuit and transformers by an ideal voltage transformer in series with an impedance. Once the loads, active and reactive power injections and network parameters are defined, load flow analysis solves the bus voltages and phases, after which the branch power flow can be calculated. Generators and loads represent the boundary conditions of the solution.

Mathematically, power flow requires a solution of a system of simultaneous nonlinear equations. However, with the continuous increase of power system scale, the dimension of load flow equations becomes very high, and for equations with such high dimensions, we cannot ensure that any mathematical method will arrive at the right solution. Hence choosing a reliable method is essential [1, 2].

Early in the development of the first digital computers, the most widely used method was the Gauss-Seidel iterative method, which was based on the nodal admittance matrix of the power system (the impedance matrix that represents the topology and parameters of the power network) [Stagg 1968] [3]. Although the basis for this method is rather simple and its memory requirement is relatively small, its convergence is nonetheless generally unsatisfactory.

To solve this problem, the sequential substitution method based on the nodal impedance matrix is used, which is also called the impedance method. The two main difficulties of the impedance method are [Brown 1963] [4]:

- High memory requirement, and
- Computing burden.

The first solution for overcoming the disadvantages of the impedance method is a piecewise solution of the impedance matrix load flow. It presents a method which involves splitting a power system into pieces to permit the use of the impedance matrix method on large systems. This method retains the same features and convergence characteristics of the impedance method [Andretich 1968] [5].
The other (and better) solution for overcoming the disadvantages of the impedance method is the Newton-Raphson method [Tinney 1967] [6], which is more widely in use.

- Its prominent features are:
- Better accuracy and reliability;
- Fewer iterations for convergence;
- Independently of the iteration number to the number of buses in the system; and
- Faster computations.

The Newton-Raphson power flow (NRPF) method is the most robust power flow algorithm in use today. Nevertheless, despite this method's popularity, load flow methods

continue to be developed. Among these, the most successful are the fast-decoupled method [Stott 1974] [7].

Compared to the Newton method, the fast-decoupled method is faster, simpler, and more efficient algorithmically and requires less storage, but it may fail to converge when some of the basic assumptions do not hold. Convergence of iterative methods depends on the dominance of the diagonal elements of the bus admittance matrix. A comparison of the convergence of the Gauss-Seidel, Newton-Raphson and the fast-decoupled method power flow algorithms are shown in figure 1. [Wood 1996] [8].

Because the Newton-Raphson method is a gradient method, it is quite complicated and therefore programming is also comparatively difficult and complicated. With this method, memory requirements are rather large, especially for large-size systems. Nonetheless, the method is versatile, reliable and accurate and best matched for load flow calculation of large-size systems [Murty 2011] [9]. Since the 1970s, research on load flow analysis has been very active. The artificial neural network algorithm [Nguyen 1995] [10] [Chan 2000] [11], the genetic algorithm [Wong 1999] [12] and Fuzzy-logic method [Lo 1999] [13] have also been the load flow analysis. However, these new models and new algorithms still cannot replace the Newton-Raphson or fast-decoupled methods. According to the literature review, because of the applicability of the Newton-Raphson method to large-size systems and its stability for convergence, this thesis implements the Newton-Raphson method for the calculation of the actual state of power system based on network parameters, power injections, and loads.

From the careful review of literature, the following objectives are formulated in this paper

- To develop a mathematical formulation to solve load flow problem in the presence of DC link in a power system using conventional NR load flow formulation.
- To identify the effect of rectifier delay angle (α) and inverter extinction angle (β) corresponds to DC transmission line on system parameters.
- To analyze the effect of AC-DC network on various power system parameters such as regulation, efficiency, corona loss, generation cost, emission, total power losses, etc.
- To analyze the effect of FACTs controllers on the above said power system parameters.

2. Load flow formulation

Power flow studies are one of the most important aspects of power system planning and operation. It gives sinusoidal steady state solution of the entire system voltages; real and reactive power generated and absorbed and line losses. Several conventional methods are used for load flow analysis such as Gauss method, Gauss Siedal method, Newton-Raphson method, Decoupled and Fast Decoupled methods, etc.

2.1 Power flow studies

Power flow study is the steady-state analysis of an interconnected power system during normal operating conditions. To obtain a complete description of the behavior of the power system, it is essential to know the voltages at various buses and the power flowing through the elements of the system. This study also help the planning and operation engineers to meet the contingency situations such as loss of a large generating unit or a major line outage due to thermal over loading of the line. Usually, the system is

assumed to be operating under balanced conditions and hence can be represented by a single-phase network.

In practical only polar form is used because it results in a smaller number of equations than the total number of equations involved in rectangular form.

At any p^{th} bus, the voltage can be considered as $\overline{V_p} = V_p e^{j\delta_p}$ and admittance for a transmission connected between buses p and q can be considered as

$$\overline{Y_{pq}} = Y_{pq} e^{j\theta_{pq}}$$

Where, δ_p is the voltage angle and θ_{pq} is an admittance angle.

From this, the complex power at p^{th} bus can be calculated as

$$S_p = P_p - jQ_p \tag{2.1}$$

Where, P_p and Q_p are the real and reactive powers at the pth bus and these values can be calculated as

$$P_p = V_p^2 Y_{pi}\cos\theta_{pi} + V_p V_i \cos\left(\theta_{pi} + \delta_p - \delta_i\right) \quad ; \quad \forall\ i = 1,2,3,\mathrm{K}\, n \tag{2.2}$$

$$Q_p = V_p^2 Y_{pi}\sin\theta_{pi} + V_p V_i \sin\left(\theta_{pi} + \delta_p - \delta_i\right) \quad ; \quad \forall\ i = 1,2,3,\mathrm{K}\, n \tag{2.3}$$

2.2 Newton Raphson Power Flow solution for AC-DC power systems

In the literature, high voltage DC transmission is now an acceptable alternative to AC and is proving an economical solution not only for long distance transmission but also for underground and submarine transmission. It also serves as a means to interconnect systems of different frequencies or to deal with problems of stability or fault levels [Arnold1990] [14].

The growing number of schemes in existence and under consideration demands corresponding modelling facilities for planning and operational purposes. The basic load flow has to be substantially modified to be capable of modelling the operating state of the combined AC and DC systems under the specified conditions of load, generation, and DC system control strategies [Arnold1990] [15]. [Arrillaga 1978, 1980 and 1977] [16] [17] [18] combine the converter equations along with the AC-DC power flow equations in order to solve the combined set simultaneously.

On the other hand, [Reeves 1977 and 1973] [19] [20] solves the AC power flow equations first and then solve the DC system equations using the interface variables as computed from the AC load flow. The computed active and reactive power consumption at the converter terminals are then forced into the AC system as loads. This process continues until convergence is achieved. [El Marsafawy and Mathur 1980] [21] solve the DC system equations in a step-by-step manner and force the DC corrections in the solution of the AC system, with the process continuing until sufficient convergence is achieved.

2.3 Mathematical modeling of AC-DC load flow problem

HVDC converters included in the load flow analysis of power systems have been modeled in the polar coordinate form. An HVDC converter connected to an AC bus bar 'i' and a DC bus bar 'k'.

All model equations are given by [Arrillaga and Arnold1990] [15]; [Q. F. Ding et.al 1997] [22]:-

The DC voltage at converter station k is:

$$V_{dk} = \left(K_1 T_k |V_i| \cos\theta_k - \frac{3}{\pi} X_{ck} I_{dk}\right) (sgn)_k$$

Where $|Vi|$ = AC terminal Voltage

Tk = Converter transformer taps ratio

Xck = Commutating reactance

Idk = DC current

$K1 = \frac{3\sqrt{2}}{\pi}$

$(sgn)_k$ =1 if the converter at the AC bus bar 'i' is a rectifier.

=-1 if the converter at the AC bus bar 'i' is an inverter.

Θ_k= Converter control angle.

$\Theta_k = \alpha_k$; For rectifier operation.

$\Theta_k = \gamma_k$; For inverter operation.

$\Theta_k = \Phi_k$; for rectifying mode.

$\Phi_k = (\pi - \emptyset k)$; for inverting mode.

G is a conductance matrix of MTDC system.

All the angles are calculated by degree.

For the AC line current of the inverter transformers with converter station k, we can write the relation as

$$Ii = Ti3\sqrt{2}/\pi Idk$$

If the AC current is $1/\sqrt{3}$times the DC current, we have

$$Iac = 1/\sqrt{3} Idc$$

The DC network equations are obtained as:

$$Idk = [G]Vdk$$

The variables $Pi\ (dc)$ and $Qi\ (dc)$ are calculated by:

$$Pi\ (dc) = Pdk$$

$$Pi\ (dc) = (sgn)1|Vi\ |Idk \cos \Phi k$$

$$Qi\ (dc) = (sgn)1|Vi\ |Idk \sin \Phi k$$

$$Pdk = Vdk\ Idk$$

$$Qdk = 0$$

The active and reactive power flow from the bus i to all converter stations connected to it k is

$$Pi\ (dc) = K1|Vi\ |\ \sum_{k=1}^{n}(\text{sgn})\text{k Idk cos } \Phi\text{k}$$

$$Qi\ (dc) = \text{K1}|\text{Vi}\ |\sum_{k=1}^{n} \text{T}_\text{k}\text{Idk sin } \Phi\text{k}$$

These equations, with new injected power-Pd and -Qd can be written as

$$Psch - Pcal\ (AC) - Pcal\ (DC) = 0$$

$$Qsch - Qcal\ (AC) - Qcal\ (DC) = 0$$

Where:

$Psch$: is the AC system load on the bus bar.

$Pcal\ (AC)$: is the injected power at the terminal busbar as a function of the AC system variables.

$Psch(DC)$: is the injected power at the terminal Busbar as a function of the DC system variables.

And similarly, $Qsch$, $Qcal\ (AC)$ and $Qsch(DC)$.

The injected powers $Psch(DC)$, and $Qsch(DC)$ are the functions of the converter, AC terminal bus bar voltage and of the DC system variables. So, we have

$$Psch(DC) = R(V, Udc\ )$$

$$Qsch(DC) = R(V, Udc\ )$$

2.3.1 Evaluation of Derivatives

The diagonal and off-diagonal elements for each of the sub-matrices in the Jacobian matrix are given below:

A sub matrix

$$\text{J}_1 = \frac{\partial \text{P}}{\partial \delta}$$

$$\frac{\partial \text{P}_\text{i}}{\partial \delta_\text{i}} = -\text{Q}_{\text{i,cal}}(|\text{V}|, \delta) - \text{B}_{\text{ii}}|\text{V}_\text{i}|^2$$

$$\frac{\partial \text{P}_\text{i}}{\partial \delta_\text{j}} = -|\text{V}_\text{j}\text{V}_\text{i}\text{Y}_{\text{ij}}|\sin(\theta_{\text{ij}} + \delta_\text{j} - \delta_\text{i})$$

B sub matrix

$$\text{J}_4 = |\text{V}|\frac{\partial \text{P}}{\partial |\text{V}|}$$

$$|\text{V}_\text{i}|\frac{\partial \text{Q}_\text{i}}{\partial |\text{V}_\text{i}|} = -\frac{\partial \text{P}_\text{i}}{\partial \delta_\text{i}} - 2\text{B}_{\text{ii}}|\text{V}_\text{i}|^2$$

$$|\text{V}_\text{j}|\frac{\partial \text{Q}_\text{i}}{\partial |\text{V}_\text{j}|} = +\frac{\partial \text{P}_\text{i}}{\partial \delta_\text{j}}$$

$$|\text{V}_\text{i}|\frac{\partial \text{Q}_\text{i}}{\partial |\text{V}_\text{i}|} = -\frac{\partial \text{P}_\text{i}}{\partial \delta_\text{j}} - 2\text{B}_{\text{ii}}|\text{V}_\text{i}|^2 + \text{Q}_{\text{i,cal}}(|\text{V}|, \text{U}_{\text{dc}})$$

$$|V_j|\frac{\partial Q_i}{\partial |V_j|} = +\frac{\partial P_i}{\partial \delta_j}$$

C sub matrix

$$J_3 = \frac{\partial Q}{\partial \delta}$$

$$\frac{\partial Q_i}{\partial \delta_i} = P_{i,cal}(|V|,\delta) - G_{ii}|V_i|^2$$

$$\frac{\partial Q_i}{\partial \delta_j} = -|V_i V_i Y_{ij}|\cos(\theta_{ij} + \delta_i - \delta_i)$$

D sub matrix

$$J_2 = |V|\frac{\partial P}{\partial |V|}$$

$$|V_i|\frac{\partial P_i}{\partial |V_i|} = \frac{\partial Q_i}{\partial \delta_i} + 2G_{ii}|V_i|^2$$

$$|V_j|\frac{\partial P_i}{\partial |V_j|} - |V_j V_i Y_{ij}|\cos(\theta_{ij} + \delta_j - \delta_i) - -\frac{\partial Q_i}{\partial \delta_i}$$

$$|V_j|\frac{\partial P_i}{\partial |V_j|} - |V_j V_i Y_{ij}|\cos(\theta_{ij} + \delta_j - \delta_i) - -\frac{\partial Q_i}{\partial \delta_i}$$

$$|V_i|\frac{\partial P_i}{\partial |V_i|} = -\frac{\partial Q_i}{\partial \delta_i} - 2G_{ii}|V_i|^2 + P_{i,cal}(|V|, U_{dc})$$

3. Modeling of FACTs Controllers and Implementation Methodology

At present, power system operation, control, management becomes very complex due to continuously increasing demand and the power flow over the transmission lines. Usually power is transferred over a long distances in an interconnected systems. This task is more complicated and needs a proper coordination between various controllers and systems.

As power transfers increase, the operation of power system has become gradually more complex and the power system can be less secure. The transmission line can operate at its maximum limits with the incorporation of FACTS controllers. These devices improves the system stability, reduces the power flows in the heavily loaded lines by controlling transmission line parameters and system control variables such as current, voltage and phase angles at system buses. These controllers provide great flexibility under normal as well as contingency conditions [23-26].

By controlling voltage magnitude and phase angles at system buses using FACTS controllers, the system losses can be reduced. Similarly, the power flows in transmission lines can be controlled using these devices [27, 28].

From the careful review of the literature, it is identified that, power flow in transmission lines can be varied using series FACTS controllers. In this work, modeling of thyristor controlled series capacitor (TCSC) is presented with equivalent power injections. The optimal location of this device is identified using contingency analysis through performance index and severity index calculations. Total cost

objective function is formulated by combining fuel cost and TCSC investment cost functions. This cost objective is solved while satisfying system and practical constraints using ICA algorithm. The proposed methodology is tested on standard IEEE test systems.

3.1 SERIES FACTS CONTROLLERS

Better utilization of existing power system capacities by installing new power electronic controllers such as FACTS has become imperative. These FACTS controllers can operate in fast and more efficiently towards obtaining better performance of a give system. These FACTs controllers can control phase angle, voltage magnitudes at system buses and active and reactive power flows in transmission lines to operate system safely and effectively by controlling system line impedance.

3.1.1 Operating principle of TCSC

The most popular variable impedance type series FACTS controller is thyristor controlled series controller. This controller is used to control the power flow in transmission line, where it is connected. The simple structure of TCSC is shown in Fig.3.1. This basic structure consists, anti parallel connected capacitor and thyristor controlled series reactor (TCR). Using this device, by varying the net impedance of the transmission line, the power flow in transmission line is controlled. This device is most popularly used device as its construction and operation is simple when compared to other series controllers.

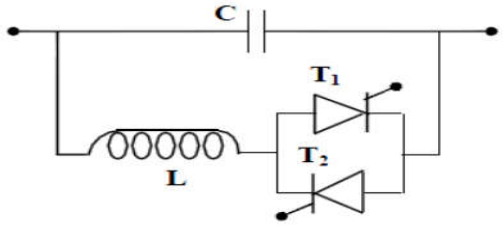

Fig.3.1 Model of TCSC

To analyze the effect of this device, TCSC should be incorporated in a given system. For this, power injection model of this device is described as follows:

A simple transmission system represented π-equivalent parameters connected between bus-s and bus-r. The real and reactive power flows from bus-s to bus-r can be written as

$$P_{sr} = V_s^2 G_{sr} - V_s V_r [G_{sr} Cos(\delta_{sr}) + B_{sr} Sin(\delta_{sr})] \quad (3.1)$$

$$Q_{sr} = -V_s^2 (B_{sr} + B_{sh}) - V_s V_r [G_{sr} Sin(\delta_{sr}) - B_{sr} Cos(\delta_{sr})] \quad (3.2)$$

Where $\delta_{sr} = \delta_s - \delta_r = -\delta_{rs}$

The real and reactive power flows from bus-r to bus-s is

$$P_{rs} = V_r^2 G_{sr} - V_s V_r [G_{sr} Cos(\delta_{sr}) - B_{sr} Sin(\delta_{sr})] \quad (3.3)$$

$$Q_{rs} = -V_r^2 (B_{sr} + B_{sh}) + V_s V_r [G_{sr} Sin(\delta_{sr}) + B_{sr} Cos(\delta_{sr})] \quad (3.4)$$

3.1.2 Power Injection Model of TCSC

Fig. 3.2 shows a π model of transmission line with TCSC connected between bus-s and bus-r. Under the steady state condition, the TCSC can be represented as a

static reactance $-jX_C$. In the power flow equations, the controllable reactance X_C is directly used as the control variable.

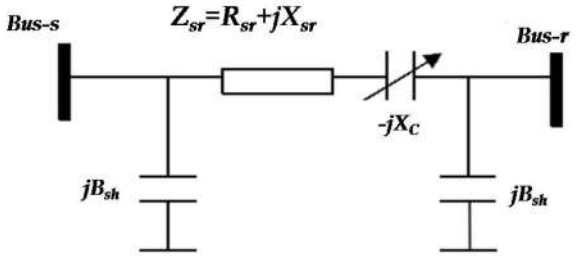

Fig.3.2 Transmission line with TCSC

The line data will be modified by placing TCSC in series with line. A new line reactance is given as follows

$$X_{sr\,new} = X_{sr} - X_C \tag{3.5}$$

Therefore new line admittance between buses s and r can be derived as follows

$$Y'_{sr} = \frac{1}{Z'_{sr}} = \frac{1}{R_{sr} + j(X_{sr} - X_C)} \; ; \quad Y'_{sr} = G'_{sr} + jB'_{sr} = \frac{R_{sr} - j(X_{sr} - X_C)}{R_{sr}^2 + (X_{sr} - X_C)^2}$$

$$G'_{sr} = \frac{R_{sr}}{R_{sr}^2 + (X_{sr} - X_C)^2} \tag{3.6}$$

$$B'_{sr} = -\frac{(X_{sr} - X_C)}{R_{sr}^2 + (X_{sr} - X_C)^2} \tag{3.7}$$

The modified active and reactive power flows from bus-s to bus-r, and from bus-r to bus-s of a line having series impedance and a series reactance are

$$P_{sr}^{TCSC} = V_s^2 G'_{sr} - V_s V_r \left(G'_{sr} Cos(\delta_{sr}) + B'_{sr} Sin(\delta_{sr})\right) \tag{3.8}$$

$$Q_{sr}^{TCSC} = -V_s^2 \left(B'_{sr} + B_{sh}\right) - V_s V_r \left(G'_{sr} Sin(\delta_{sr}) - B'_{sr} Cos(\delta_{sr})\right) \tag{3.9}$$

$$P_{rs}^{TCSC} = V_r^2 G'_{sr} - V_s V_r \left(G'_{sr} Cos(\delta_{sr}) - B'_{sr} Sin(\delta_{sr})\right) \tag{3.10}$$

$$Q_{rs}^{TCSC} = -V_r^2 \left(B'_{sr} + B_{sh}\right) + V_s V_r \left(G'_{sr} Sin(\delta_{sr}) + B'_{sr} Cos(\delta_{sr})\right) \tag{3.11}$$

The power loss in the line with TCSC can be written as

$$P_{Loss} = P_{sr}^{TCSC} + P_{rs}^{TCSC} = G'_{sr}\left(V_s^2 + V_r^2\right) - 2V_s V_r G'_{sr} Cos(\delta_{sr}) \tag{3.12}$$

$$Q_{Loss} = Q_{sr}^{TCSC} + Q_{rs}^{TCSC} = -\left(V_s^2 + V_r^2\right)\left(B'_{sr} + B_{sh}\right) + 2V_s V_r B'_{sr} Cos(\delta_{sr}) \tag{3.13}$$

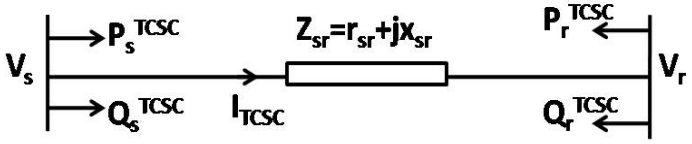

Fig.3.3 Power injection model of TCSC

Due to TCSC, the change in line flow can be represented as a line without TCSC plus with power injected at the sending and receiving ends of the line with device as shown in Fig. 3.3. The active and reactive power injections at bus-s and bus-r can be written as

$$P_s^{TCSC} = P_{sr} - P_{sr}^{TCSC} = V_s^2 \Delta G_{sr} - V_s V_r \left[\Delta G_{sr} \mathrm{Cos}\left(\delta_{sr}\right) + \Delta B_{sr} \mathrm{Sin}\left(\delta_{sr}\right)\right] \quad (3.14)$$

$$P_r^{TCSC} = P_{rs} - P_{rs}^{TCSC} = V_s^2 \Delta G_{sr} - V_s V_r \left[\Delta G_{sr} \mathrm{Cos}\left(\delta_{sr}\right) - \Delta B_{sr} \mathrm{Sin}\left(\delta_{sr}\right)\right] \quad (3.15)$$

$$Q_s^{TCSC} = Q_{sr} - Q_{sr}^{TCSC} = -V_s^2 \Delta B_{sr} - V_s V_r \left[\Delta G_{sr} \mathrm{Sin}\left(\delta_{sr}\right) - \Delta B_{sr} \mathrm{Cos}\left(\delta_{sr}\right)\right] \quad (3.16)$$

$$Q_r^{TCSC} = Q_{rs} - Q_{rs}^{TCSC} = -V_r^2 \Delta B_{sr} + V_s V_r \left[\Delta G_{sr} \mathrm{Sin}\left(\delta_{sr}\right) + \Delta B_{sr} \mathrm{Cos}\left(\delta_{sr}\right)\right] \quad (3.17)$$

Where

$$\Delta G_{sr} = \frac{X_C R_{sr}\left(X_C - 2X_{sr}\right)}{\left(R_{sr}^2 + X_{sr}^2\right)\left(R_{sr}^2 + \left(X_{sr} - X_C\right)^2\right)}, \quad \Delta B_{sr} = \frac{-X_C\left(R_{sr}^2 - X_{sr}^2 + X_C X_{sr}\right)}{\left(R_{sr}^2 + X_{sr}^2\right)\left(R_{sr}^2 + \left(X_{sr} - X_C\right)^2\right)}$$

TCSC device is modeled with power injection model so far by using the TCSC control variable. It is possible to calculate the complex power injected S_s^{TCSC} and S_r^{TCSC} at bus-s and bus-r respectively.

$$S_s^{TCSC} = P_s^{TCSC} + jQ_s^{TCSC}, \quad S_r^{TCSC} = P_r^{TCSC} + jQ_r^{TCSC}$$

Then, new power flow equations can be expressed by the following relationship

$$\begin{bmatrix} \Delta P \\ \Delta Q \end{bmatrix} = \begin{bmatrix} H_{new} & M_{new} \\ N_{new} & L_{new} \end{bmatrix} \cdot \begin{bmatrix} \Delta\delta \\ \frac{\Delta V}{V} \end{bmatrix}$$

Where, new mismatch vectors are

$$\Delta P_i = P_i^{spec} + P_i^{TCSC} - P_i^{Calc}; \forall\, i = s,r$$

$$\Delta Q_i = Q_i^{spec} + Q_i^{TCSC} - Q_i^{Calc}; \forall\, i = s,r$$

P_i^{spec} and Q_i^{spec} are the classical specified real and reactive powers, P_i^{TCSC} and Q_i^{TCSC} are the power injection associated to TCSC devices, P_i^{calc} and Q_i^{calc} are computed using the power flow equations. Now, modified Jacobian matrix due to power injections of TCSC

$$H_{new} = H + \frac{\partial P_i^{TCSC}}{\partial\delta} \quad \forall\, i = s,r; \quad M_{new} = M + \frac{\partial P_i^{TCSC}}{\partial V} V \quad \forall\, i = s,r$$

$$N_{new} = N + \frac{\partial Q_i^{TCSC}}{\partial\delta} \quad \forall\, i = s,r; \quad L_{new} = L + \frac{\partial Q_i^{TCSC}}{\partial V} V \quad \forall\, i = s,r$$

H, M, N and L are the classic sub-Jacobian matrices.

3.2 STATIC VAR COMPENSATOR (SVC)

The IEEE definition of the SVC is as follows: "A shunt connected static VAr generator or absorber whose output is adjusted to exchange capacitive or inductive current so as to maintain or control specific parameters of the electrical power system (typically bus voltage)."

SVCs are used in a given power systems to enhance the voltage levels so that system stability has been improved.

3.2.1 Modeling of SVC

In practice, the SVC can be seen as an adjustable reactance with either firing-angle limits or reactance limits. The equivalent circuit shown in Fig. 5.1 is used to derive the SVC nonlinear power equations. With reference to Fig. 5.1, the current drawn by the SVC is

$$I_{SVC} = jB_{SVC}V_i . \tag{3.18}$$

And the reactive power drawn by the SVC, which is also the reactive power injected at bus-i, is

$$Q_{SVC} = Q_i = -V_i^2 B_{SVC} . \tag{3.19}$$

It is a bank of three-phase static capacitors and/or inductors. Under heavy loading conditions, when positive VAr is needed, capacitor banks are needed, when negative VAr is needed, inductor banks are used. In this thesis, SVC is modeled as an ideal reactive power injection at bus-i shown in Fig.3.4.

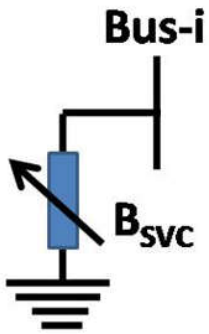

Fig.3.4 Power injection model of SVC

3.3 POWER SYSTEM PERFORMANCE PARAMETERS

This section explains about various electrical parameters of power system and its impact on the power system parameters.

Generation fuel cost

The total amount of power generation should meet the demand at lowest fuel cost. The total fuel cost function can be expressed mathematically in the following form m

$$FC = \sum_{i=1}^{NG} C_i(P_{Gi}) \qquad \$/h$$

where, 'FC' is the total generation fuel cost, '$C_i(P_{Gi})$' is the fuel cost function of the i^{th} unit, 'P_{Gi}' is the power generated by the i^{th} unit and 'NG' is

the total number of generating units. This objective function is modeled as quadratic fuel cost function

The quadratic fuel cost of a thermal generating unit in the form of second order polynomial function can be represented using

$$C_i(P_{Gi}) = a_i P_{Gi}^2 + b_i P_{Gi} + c_i \qquad \$/hr \tag{3.20}$$

where, a_i, b_i, and c_i are the fuel-cost coefficients of the i^{th} unit,

Emission objective

The emission of gasses in the boiler is represented as the sum of various gasses emitted such as NO_2, SO_2, thermal emission, etc. The amount of the gasses emitted is the function of generator output given by,

$$A_2 = \min\left[E(P_{G_i})\right] = \sum_{i=1}^{NG} e_i \quad (ton/h) \tag{3.21}$$

where e_i is the emission of the i^{th} generator

The emission curve is represented in quadratic function as

$$e_i = \alpha_i + \beta_i P_{Gi} + \gamma_i P_{Gi}^2 + \xi_i \exp(\lambda_i P_{Gi}) \ (ton/h) \tag{3.22}$$

Where $\alpha_i, \beta_i, \gamma_i, \xi_i$ and λ_i are the emission coefficients of the i^{th} generator

Total Power Losses

The objective function used to calculate the total power loss (TPL). Power loss through a line is a function of power flow through it, which can be obtained from power flow solution. The power loss can be expressed as,

$$A_3 = \min(TPL) = \sum_{i=1}^{nl} P_{Loss\ i} \tag{3.23}$$

Where P_{Loss_i} is the real power loss in i^{th} line

Transmission Line Voltage Regulation

Voltage regulation of transmission line is defined as the ratio of difference between sending and receiving end voltage to receiving end voltage of a transmission line between conditions of no load and full load. It is also expressed in percentage.

$$\%VR = \frac{V_S - V_R}{V_R} \times 100 \tag{3.24}$$

Where, Vs is the sending end voltage per phase and VR is the receiving end voltage per phase.

$$V_S = \sqrt{(V_R \cos\theta_R + IR)^2 + (V_R \sin\theta_R + IX_L)^2}$$

X_L is the reactance per phase

R is the resistance per phase

Cos θ_R is the receiving end power factor

Transmission Efficiency

Transmission efficiency is defined as the ration of receiving end power P_R to the sending end power P_S and it is expressed in percentage value.

$$\%\,\eta T = \frac{P_R}{P_S} \times 100 \qquad (3.25)$$

Corona loss

Formation of corona is always accompanied by energy loss. which is dissipated in the form of light, heat, sound and chemical action. When disruptive voltage is exceeded, the power loss due to corona is given by :

$$P = 241(f+25)\sqrt{\frac{r}{d}}\left[V_0 - 21.1K_i r \ln\left(\frac{d}{r}\right)\right]^2 \times 10^{-5} \quad \text{kW/km} \qquad (3.26)$$

F=frequency in Hz

4. Results and Analysis

The effectiveness of the developed methodology is tested on IEEE-14 bus test system [Ref]. This system consist fourteen buses, twenty one transmission lines, five generators located at buses, 1, 2, 3, 6 and 8, one shunt compensator located at bus-9 and three tap changing transformers installed in the lines 8 (4-7), 9 (4-9) and 10 (5-6). The total active and reactive power loads are 246.05 MW and 69.825 MVAr respectively. To formulate AC-DC network, 13th transmission line i.e. connected between buses 7 and 9 is assumed to be the DC link. In this line, the rectifier is connected at bus-7 and inverter is connected at bus-9.

The entire analysis is performed for the following modules:

Module-1: Identifying the effectiveness of AC-DC network over conventional AC network.

Module-2: Analyzing the effect of converter parameters such as rectifier delay angle (α) and inverter extinction angle (β) on system parameters. For this, these angles are varied from 0 deg to 360 deg in steps of 20 deg.

Module-3: Analyzing the effect of AC-DC load flow on various power system parameters.

Module-4: Analyzing the effect of FACTs controllers such as SVC and TCSC on various power system parameters when compared to without device.

4.1 Module-1

In this module, both NR load flow problem is solved for the AC network and AC-DC networks. To identify the effect of DC link on system parameters, the rectifier delay angle (α) and inverter extinction angle (β) are assumed to be 60 deg and 220 deg respectively. The obtained load flow results for the voltage magnitude and voltage angles are tabulated in Table.4.1. From this, it is identified that, the voltage magnitude at bus-7 is enhanced and bus-9 is decreased. This is due to operation of $\alpha < 180$ deg and $\beta > 180$ deg. The variation of voltage magnitudes and voltage angles are shown in Figs. 4.1 and 4.2.

Table.4.1 Voltages with AC-DC NR load flow method for IEEE-14 bus system

Bus No	VM, p.u.		VA, deg	
	AC NR	AC-DC NR	AC NR	AC-DC NR
1	1.06	1.06	0	0
2	1.045	1.045	-2.312	-2.243
3	1.011	1.012	-6.012	-5.866
4	1.024	1.024	-5.945	-5.844
5	1.026	1.026	-4.98	-4.93
6	1.07	1.07	-8.048	-8.244
7	1.064	1.065	-7.781	-7.264
8	1.09	1.09	-6.911	-6.395
9	1.057	1.053	-9.299	-9.756
10	1.052	1.049	-9.35	-9.76
11	1.058	1.056	-8.828	-9.131
12	1.056	1.056	-8.898	-9.115
13	1.051	1.051	-9.016	-9.249
14	1.038	1.035	-10.124	-10.487

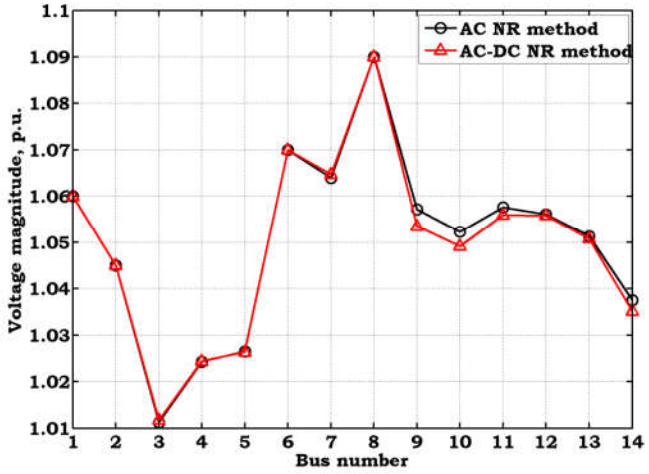

Fig.4.1 Variation of voltage magnitude with AC-DC NR load flow method for IEEE-14 bus system

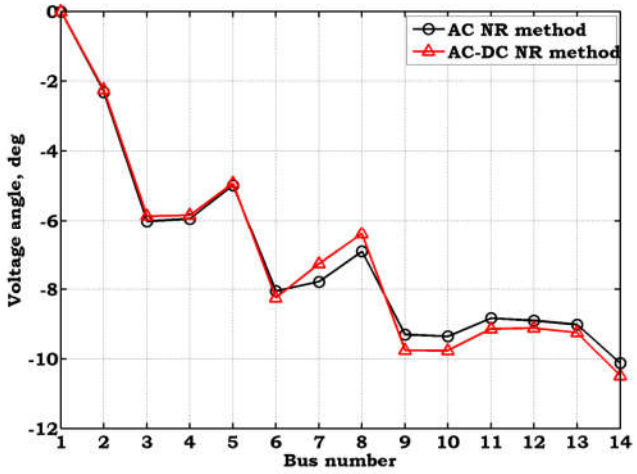

Fig.4.2 Variation of voltage angle with AC-DC NR load flow method for IEEE-14 bus system

Similarly, the power flow results are tabulated in Table.4.2. From this result, it is identified that, power flow through DC link is decreased from 27.95 MVA to 23.909 MVA. The variation of power flow is shown in Fig.4.3.

Table.4.2 Power flows with AC-DC NR load flow method for IEEE-14 bus system

Line No	Power flow, MVA	
	AC NR	AC-DC NR
1	76.618	74.547
2	44.28	43.896
3	37.687	36.943
4	38.723	38.407
5	29.421	29.636
6	8.871	8.638
7	40.226	38.066
8	18.875	15.72
9	11.759	13.71
10	28.866	30.64
11	9.261	10.513
12	7.934	8.101
13	18.945	19.602
14	18.577	18.19
15	27.95	23.909
16	5.845	5.068
17	8.755	7.993
18	5.536	6.732
19	1.842	2.003
20	6.633	7.429

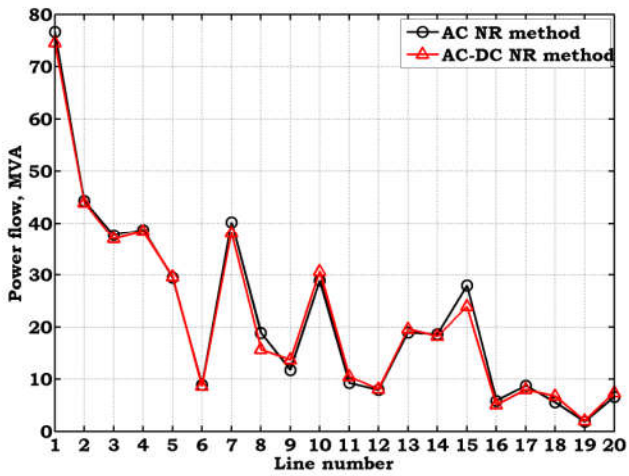

Fig.4.3 Variation of power flow with AC-DC NR load flow method for IEEE-14 bus system

Further, the active and reactive power losses, number of iterations, time taken for convergence results are tabulated in Table.4.3. From this table, it is identified that, the total active power losses are decreased with the incorporation of DC link in AC network. Similarly, the total number of iterations is also decreased. Due to complexity in computation, the time taken for convergence is increased.

Table.4.3 Power losses and performance parameters with AC-DC NR load flow method for IEEE-14 bus system

Parameters	AC NR	AC-DC NR
Active power losses, MW	4.635	4.563
Reactive power losses, MVAr	-8.665	-8.441
Number of Iterations	5	4
Time, Sec	0.053	0.097

4.2 Module-2

Further, to analyze the effect of DC link converters on system performance, the analysis is performed by varying rectifier delay angle (α) and inverter extinction angle (β). For this, these angles are varied from 0 deg to 360 deg in steps of 20 deg.

For each step of angles variation, the minimum and maximum voltage magnitude at buses along with respective α and β values are tabulated in Table.4.4. From this table, it is observed that, the generator connected at bus-3 is no longer PV bus due to the rectifier operation at bus-5. It is also observed that, maximum difference is obtained at bus-3 and minimum difference is obtained at bus-12. The variation of voltage difference at buses is shown in Fig.4.4.

Table.4.4 Variation of voltage magnitudes with AC-DC NR load flow method for IEEE-14 bus system

Bus No	V_{min} (p.u.)	α (deg)	β (deg)	V_{max} (p.u.)	α (deg)	β (deg)	V_{diff} (p.u.)
1	1.06	0	0	1.06	0	0	0
2	1.045	0	0	1.045	0	0	0
3	1.01	0	80	1.012	60	240	-0.0028
4	1.024	60	80	1.025	0	240	-0.0007
5	1.026	60	80	1.026	0	240	-0.0004
6	1.07	0	0	1.07	0	0	0
7	1.065	60	80	1.065	0	240	-0.0003
8	1.09	0	0	1.09	0	0	0
9	1.053	0	180	1.054	60	20	-0.0003
10	1.049	0	180	1.049	60	20	-0.0002
11	1.056	0	180	1.056	60	20	-0.0001
12	1.056	60	80	1.056	0	240	-2E-05
13	1.051	0	180	1.051	60	20	-4E-05
14	1.035	0	180	1.035	60	20	-0.0002

$V_{diff}=V_{max}-V_{min}$

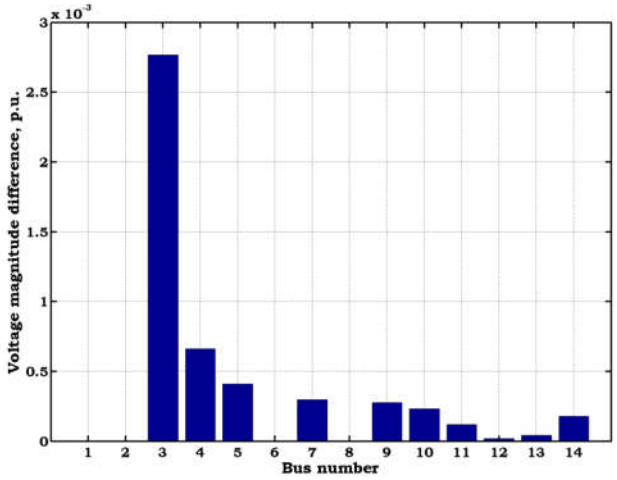

Fig.4.4 Variation of voltage difference with AC-DC NR load flow method for IEEE-14 bus system

Similarly, for each step of angles variation, the minimum and maximum power flow in transmission lines along with respective α and β values are tabulated in Table.4.5. From this table, it is observed that, the first transmission line connected to slack has major variation of power flow. As the generation from slack bus is increased to divert the power to the loads. The variation of power flow difference in lines is shown in Fig.4.5.

Table.4.5 Variation of power flow with AC-DC NR load flow method for IEEE-14 bus system

Line No	S_{min} (p.u.)	α (deg)	β (deg)	S_{max} (p.u.)	α (deg)	β (deg)	S_{diff} (p.u.)
1	74.537	60	0	78.592	0	60	-4.055
2	43.895	60	0	44.967	0	60	-1.072
3	36.879	0	220	38.34	60	60	-1.461
4	38.262	0	220	38.77	60	60	-0.508
5	29.443	0	220	29.822	60	60	-0.38
6	8.308	60	240	9.444	0	80	-1.136
7	38.06	60	0	39.018	0	160	-0.958
8	15.679	0	140	15.775	60	80	-0.096
9	13.679	0	280	13.711	60	120	-0.032
10	30.605	60	300	30.692	0	140	-0.088
11	10.511	60	120	10.556	0	280	-0.045
12	8.1	60	340	8.107	0	180	-0.007
13	19.6	60	120	19.626	0	180	-0.025
14	18.149	0	240	18.295	60	80	-0.146
15	23.875	0	280	23.909	60	220	-0.034
16	5.027	0	80	5.083	60	240	-0.056
17	7.963	0	180	7.997	60	340	-0.034
18	6.732	60	120	6.772	0	280	-0.04
19	2.003	60	340	2.01	0	180	-0.007
20	7.429	60	120	7.457	0	280	-0.028

$S_{diff}=S_{max}-S_{min}$

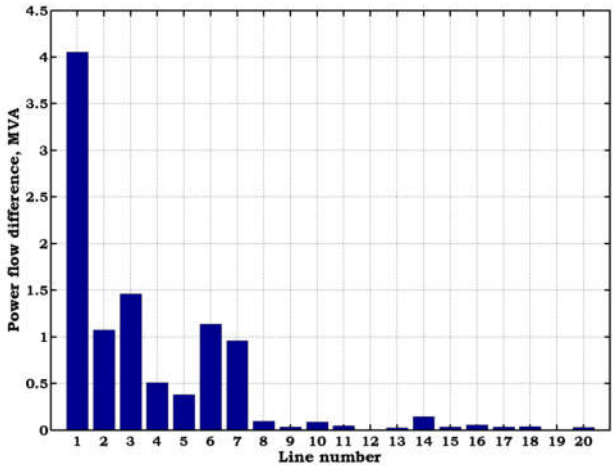

Fig.4.5 Variation of power flow difference with AC-DC NR load flow method for IEEE-14 bus system

At last, minimum and maximum power losses along with respective α and β values are tabulated in Table.4.6. From this, it is observed that, there is a power loss difference of 0.222 MW with DC link.

Table.4.6 Variation of power loss with AC-DC NR load flow method for IEEE-14 bus system

	$Ploss_{min}$ (MW)	α (deg)	β (deg)	$Ploss_{max}$ (MW)	α (deg)	β (deg)	$Ploss_{diff}$ (MW)
P loss, MW	4.562806	60	220	4.78495	0	60	0.222144

4.3 Module-3

To extend the benefit of AC-DC transmission for power system performance enhancement, certain power system parameters are considered and the corresponding results are tabulated in Table.4.7. Due to DC link, the sending and receiving end voltage magnitudes are increased, this in turn decreases the line current, power flows, total generation, generation cost, emission of flue gases and total power losses. Also, voltage regulation is decreased which increases the total transmission efficiency. It is also observed that, in AC-DC system, corona losses are decreased by 62.6053 kW when compared to AC system.

Table.4.7 Power system parameters with AC-DC NR load flow method for IEEE-14 bus system

S. No	Parameter	AC NR method	AC-DC NR method
1	Sending end voltage magnitude (V_S), p.u.	1.063954	1.064737
2	Receiving end voltage magnitude (V_r), p.u.	1.057153	1.059124
3	Line current (I_{line}), Amps	0.2433-j0.0990	0.2089-j0.0855
4	Active power flow (7-9), MW	27.07624	23.21865
5	Reactive power flow (7-9), MVAr	6.935814	5.705615
6	Apparent power flow (7-9), MVA	27.95046	23.90941
7	Total generation, MW	250.68528	250.61281
8	Generation cost, $/hr	2175.0675	2150.9896
9	Emission, ton/hr	10.639068	10.366526
10	Total power losses, MW	4.6352826	4.5628056
11	Voltage regulation of line (%)	47.5161	38.9745

12	Transmission efficiency	82.5830	82.8166
13	Corona loss (kW/km)	94.0826	31.4773

4.4 Module-4

To analyze the effectiveness of FACTs controllers on system performance, the basic variable impedance shunt (Static VAr Compensator) and series (Thyristor controlled series compensator) controllers are considered.

The shunt controller is placed at the bus which is having low voltage after performing AC-DC load flow (i.e. from Table.4.1) and which doesn't have any nearby generators support. Hence, for this system, bus-14 is considered to be the optimal location to install SVC and the size of this device is considered to be 50 MVAr. Similarly, series controller is placed in a line which is having high power flow margin (i.e. difference between rated capacity and actual power flow). For this system, line-6 i.e. connected between buses 3 and 4 is considered to be the optimal location. After that, the size of this device is considered to be 80% of transmission line reactance i.e. (0.8*Xline=0.034206).

After performing AC-DC load flow solution in the presence of SVC and TCSC individually, the results of power system parameters are tabulated in Table.4.8. From this table, it is identified that, the series and shunt compensations effects the power system parameters as per their nature of compensation.

Table.4.8 Power system parameters with SVC and TCSC for IEEE-14 bus system

S. No	Parameter	Without device	With SVC	With TCSC
1	Sending end voltage magnitude (V_S), p.u.	1.064737	1.085152	1.064074
2	Receiving end voltage magnitude (V_r), p.u.	1.059124	1.106271	1.052851
3	Line current (I_{line}), Amps	0.2089-j0.0855	0.2313+j0.0662	0.2085-j0.0855
4	Active power flow (7-9), MW	23.21865	23.94129	23.17092
5	Reactive power flow (7-9), MVAr	5.705615	-10.411	6.190107
6	Apparent power flow (7-9), MVA	23.90941	26.10697	23.98351
7	Total generation, MW	250.61281	251.79422	250.66277
8	Generation cost, $/hr	2150.9896	2177.4353	2155.329
9	Emission, ton/hr	10.366526	11.705576	10.413689
10	Total power losses, MW	4.5628056	5.7442168	4.6127721
11	Voltage regulation of line (%)	38.9745	45.9981	34.4679
12	Transmission efficiency	82.8166	87.2366	82.8055
13	Corona loss (kW/km)	31.4773	34.3264	31.1075

5. Conclusions

From the careful review of the literature, it has been notified that, transferring power through DC link yields better system performance when compared to conventional AC transmission. To verify this, a new load flow approach to perform AC-DC load flow solution has been developed. In this, the sending end rectifier and receiving end inverters are modeled in such a way that, the effect of DC transmission has been considered in the AC load flow problem.

In this paper, a complete mathematical formulation to solve AC-DC load flow problem has been presented with supporting load flow incorporation procedure. From the analysis, it has been identified that, due to DC transmission, overall system performance has been enhanced in terms of voltage profile, decreased total losses, etc. Further, the effect of rectifier delay angle and inverter extinction angles on power system parameters such as voltage magnitude, voltage angle, power flow and total system losses has been

analyzed. From this analysis, it has been identified that, there has been a significant variation of voltage profile near by the buses where DC link is connected.

Finally, effect of FACTs controllers on AC-DC system performance in terms of power losses, generation cost, emission, voltage regulation, transmission efficiency, corona losses, etc have been analyzed. From this analysis, it has been identified that, there has been significant enhancement of system performance in the presence of FACTs controller on AC-DC power system when compared to AC power system.

References

[1] W. Xi-Fan, S. Yonghua and I. Malcolm, Modern Power Systems Analysis, lSBN 978- 0-387-72852-0, 2009.

[2] G. John and S. William, Power System Analysis, Mcgraw-Hill: lSBN 0-07-061293-5, 1994.

[3] Glenn W. Stagg, Ahmed H. El-Abiad, Computer Methods in Power Systems, Mcgraw-Hill, 1968.

[4] H. E. Brown, G. K. Carter, H. H. Happ and C. E. Person, "Power Flow. Solution By Impedance Matrix Method," IEEE Trans. Power Apparatus and System, April 1963.

[5] Robert G. Andretich, Homxier E. Brown, Harvey H. Happ and Conrad E. Person, "The Piecewise Solution of The Impedance Matrix Load Flow," IEEE Transactions on Power Apparatus And Systems, October 1968,Vol. PAS-87, No. 10, pp.1877-1882.

[6] William F. Tinney and Clifford E. Hart, "Power Flow Solution By Newton's Method," IEEE Transactions On Power Apparatus And Systems, Nov. 1967.

[7] Stott. B. and Alasc. O., "Fast Decoupled Load Flow," IEEE Transactions On Power Apparatus And Systems, PAS-93, pp.859-869, 1974.

[8] J. W. Allen and F. W. Bruce, power Generation, Operation, And Control, Wiley, ISBN:978-0471586999, 1996.

[9] P. S. R. Murty, Operation And Control In Power Systems, Taylor And Francis: ISBN: 9780415665650, 2011.

[10] T. Nguyen, "Neural Network Load-Flow," IEEE Proceedings of Generation Transmission Distribution, Vol. 142, No. 1, Jan. 1995, pp. 51-58.

[11] W. L. Chan, A. T. P. So and L. L. La, "Initial Applications Of Complex Artificial Neural Networks To Load-Flow Analysis," IEEE Proceedings Of Generation Transmission Distribution,Vol. 147, No. 6, July 2000, pp. 361-366.

[12] K. P. Wong, A. Li and T. M. Y. Law, " Advanced Constrained Genetic Algorithm Load Flow Method," IEE Proceedings Of Generation Transmission Distribution, Vol.146, No.6, November 1999, pp.609-616.

[13] K. L. Lo, Y. J. Lin and W. H. Siew, " Fuzzy-Logic Method For Adjustment Of Variable Parameters in Load Flow Calculation," IEE Proceedings of Generation Transmission Distribution, 146(3), 276–282, 1999.

[14] Ray Daniel Zimmerman, Carlos Edmundo Murillo-Sánchez and Robert John Thomas "Matpower: Steady-State Operations, Planning And Analysis Tools For Power Systems Research And Education," IEEE Transactions on Power Systems, Feb. 2011.

[15] Arrillaga, J.; Arnold, C., Computer Analysis of Power Systems, London: John Wiley and Sons Ltd, 1990.

[16] Arrillaga, J. and Bodger, P. , "AC-DC load flows with a realistic representation of converting plant," Proc. IEEE, Vol. 125, No.1, January 1978, pp. 41-46.

[17] Arritlaga, J. ; Harker, B.J. ; Turner, K.S. , "Clarifying an Ambiguity in recent ACDC load flow formulations," Proc. IEEE, Vol. 127 Pt.C., No. 5, September 1980, pp. 324-325.

[18] Arrillaga, J. ; Bodger, P. , "Integration of HVDC links with fast-decoupled load flow solutions," IEEE Proc., 124 (5), 463–468, 1977.

[19] Reeve, J. ; Fahny, G. ; Stott, B., "Versatile Load flow method for Multi-terminal HVDC Systems," IEEE Transaction Power Apparatus And Systems, 96(3), 925–932, May/June 1977.

[20] J. Reeve and J. Carr, "Review of Techniques For HVDC Multi-Terminal Systems," IEEE Int. Conference Publication, HV AC/DC Transmission, London, December 1973.

[21] El-Marsafawy, M.M. ; Mathur, R.M. , "A new technique for load flow solution of integrated multiterminal AC-DC systems," IEEE Transactions on Power Apparatus And Systems,Vol. PAS-99, No. 1, pp. 246-255, Jan./ Feb. 1980,.

[22] Ding, Q. F. ; Zhang, B. M. , "A New Approach To AC/MTDC Power Flow," Proceedings of the 4th International Conference on Advances in Power System Control, Operation and Management, Hong Kong, Vol. 2, No. 450, pp. 689-694, November 1997.

[23] M.Noroozian, L.Angquist, M.Ghandhari and G.Anderson, "Improving Power System Dynamics by Series-connected FACTS Devices", IEEE Transaction on Power Delivery, Vol.12, 1997,PP.1635-1641.

[24] M.Noroozian, L.Angquist, M.Ghandhari, and G.Anderson, "Use of UPFC for Optimal Power Flow Control", IEEE Transaction on Power Delivery, Vol.12,1997,PP.1629-1634

[25] Roy Billinton, Mahmud Fotuhi-Firuzabad, Sherif Omar Faried and Saleh Aboreshaid, "Impact of Unified Power Flow Controllers on Power System Reliability", IEEE Transaction on Power Systems Vol.15, 2000,PP.410-415

[26] James A. Momoh, Jizhong Z. Zhu, Garfiled D. Boswell and Stephen Hoffman, "Power System Security Enhancement by OPF with Phase Shifter", IEEE Transaction on Power Systems, Vol.16, 2001, PP.287-293.

[27] N. G. Hingorani and L. Gyugyi, “Understanding FACTS: Concepts and Technology of Flexible AC Transmission Systems”, IEEE Press, New- York, 2000.

[28] D. Povh “Load Flow Control in High Voltage Power Systems Using FACTS Controllers”, CIGRÉ Task Force, 1996.